

Low-lying collective excited states in non-integrable system based on stationary phase approximation to the path integral

Fang Ni,¹ Nobuo Hinohara,^{1,2} and Takashi Nakatsukasa^{1,2,3}

¹*Faculty of Pure and Applied Sciences, University of Tsukuba, Tsukuba 305-8571, Japan*

²*Center for Computational Sciences, University of Tsukuba, Tsukuba 305-8577, Japan*

³*iTHES Research Group, RIKEN, Wako 351-0198, Japan*

To describe the large amplitude collective motion in nuclear pairing, stationary phase approximation to the path integral (SPA) is supposed to be the most reliable requantization approach of time-dependent mean-field dynamics. The disadvantage of SPA is that it is only available in integrable system. However, we overcome the disadvantage by combining SPA with adiabatic self-consistent collective coordinate method (ASCC). We construct the theoretical framework of ASCC+SPA and demonstrate the application to the multi-level pairing model which is non-integrable system. As with the performance in integrable system, we find that SPA also gives reasonable information about low-lying excited 0^+ states in non-integrable system.

I. INTRODUCTION

Pairing correlation plays an important role around the surface in open-shell nuclei. The properties of pairing for the ground states are well known such as odd-even mass difference, moment of inertia of rotational bands, and the quantum numbers for spin and parity [1]. The elementary excitations of pairing, pairing vibrations and pairing rotations, are fascinating phenomena not only for open-shell nuclei, but also for closed-shell nuclei [2]. However, the pairing dynamics still has unclear features in low-energy region (a few MeV excitation) of nuclei, especially for excited $J^\pi = 0^+$ states [3, 4]. We aim to understand the dynamics from pairing correlation in nuclei from microscopic many-body theory.

Time-dependent mean-field (TDMF) theory is the common theory to describe the dynamics of nuclei from the microscopic degrees of freedom. Including pairing correlation, time-dependent Hartree-Fock-Bogoliubov (TDHFB) theory, corresponding to TDMF theory, is utilized for plenty of studies for both nuclear reaction and nuclear structure fields [5]. In nuclear structure aspect, the harmonic approximation of TDHFB, quasiparticle random phase approximation (QRPA), can well describe the giant resonance of nuclei. Recently, the adiabatic approximations of TDHFB, such as adiabatic TDHFB (ATDHFB), adiabatic self-consistent collective coordinate method (ASCC), and 5D Bohr Hamiltonian constructed from microscopic degrees of freedom, is developed and start to be applied to low-lying excited states. They are expected to elucidate the large amplitude collective motions occurred in the structure, such as shape coexistence and anharmonic vibration.

TDMF (TDHFB) theory corresponds to a stationary-limit in the path integral formulation. It lacks a part of the information about quantum fluctuation, which is remarkable in the large amplitude dynamics. To introduce the quantum fluctuation based on the TDHFB theory, the requantization process is necessary [6–11]. The straightforward requantization method is canonical quantization. In 5D Bohr Hamiltonian, the canonical quantization was formulated and employed for the study

of low-lying excited states in nuclei. In addition, it was also utilized to describe the large amplitude dynamics for pairing in pairing model [12–15]. However, the Hilbert space which the wave function obtained from canonical quantization belongs to is quite different from the Hilbert space which the original wave function belongs to. It may cause the deviation for the requantized states. In our previous work, we studied the requantization of the TDHFB. We investigated the low-lying excited 0^+ states in two-level pairing model by various requantization methods [16]. Comparing with exact solution, we found that stationary phase approximation to the path integral (SPA) [17] can give quantitatively results not only for the excitation energies, but also for the wave functions. We confirmed that SPA is superior to canonical requantization, especially for the calculation of two-particle transitional strength. The wave function obtained from SPA has two advantages: first, it is written in the (quasi)particle's degrees of freedom; second, it has good quantum number because the projection of the conservation quantities (e.g. total particle number, total angular momentum) are automatically contained. On the other hand, the disadvantage is that SPA only works in integrable systems. Due to the nuclear system is non-integrable system in general, we cannot employ SPA straightforward for the realistic system.

We discuss the application of SPA for the non-integrable system in this paper. We know that the one-dimensional system is integrable system. It is desirable that a collective motion can be described by one collective coordinate. To obtain the one-dimensional subspace, adiabatic self-consistent collective coordinate method (ASCC) is powerful tool [18]. “Adiabatic” indicates that the collective motion is slow compared with the single-particle motion. The collective degree of freedom is determined self-consistently from the TDHFB degrees of freedom without any assumption. The ASCC, which was developed from the basic idea of self-consistent collective coordinate method (SCC) [19], is flexible to deal with various collective potential, such as shape coexistence [20–22]. A state in the collective subspace corresponds to a microscopic state in TDHFB phase space connected by Q and P operators in ASCC. This correspondence make us

possible to apply SPA to non-integrable system. We construct the theoretical framework of ASCC+SPA, which implements SPA to non-integrable system by combining with ASCC. The first study of ASCC+SPA give us a new landscape about the large-amplitude dynamics in low-energy region.

The paper is organized as follows. Sec. II introduces the theoretical framework of ASCC and the combination, ASCC+SPA. Sec. III is the application of ASCC+SPA in multi-level pairing model. We give the numerical results in Sec. IV, including two-level systems, three-level systems, and Pb isotope systems. The conclusion and the remaining problems are shown in Sec. V.

II. THEORETICAL FRAMEWORK

A. One-dimensional adiabatic self-consistent collective coordinate method

To discuss the application of ASCC+SPA in the later subsection, we review the one-dimensional adiabatic self-consistent collective coordinate method (ASCC) briefly using the notation in Ref. [23]. The classical Hamilton's equation which is identical to the TDHFB equation is described by canonical variables $\{\xi^\alpha, \pi_\alpha\}$. If we apply the adiabatic approximation which assume that the collective motion is slow compared with the single-particle motion, we can expand the momenta π up to second order. The multi-dimensional Hamiltonian is

$$\mathcal{H} = V(\xi) + \frac{1}{2}B^{\alpha\beta}(\xi)\pi_\alpha\pi_\beta \quad (\text{II.1})$$

with potential $V(\xi)$ and reciprocal mass parameter $B^{\alpha\beta}(\xi)$ defined by

$$V(\xi) = \mathcal{H}(\xi, \pi = 0) \quad (\text{II.2})$$

$$B^{\alpha\beta}(\xi) = \left. \frac{\partial^2 \mathcal{H}(\xi, \pi)}{\partial \pi_\alpha \partial \pi_\beta} \right|_{\pi=0}. \quad (\text{II.3})$$

If there is a one-dimensional collective motion which is decoupled from other intrinsic motions, the collective motion can be described by a set of canonical variable $\{q, p\}$, the one dimensional collective Hamiltonian is

$$\mathcal{H}_{coll} = \bar{V}(q) + \frac{1}{2}\bar{B}^{-1}(q)p^2. \quad (\text{II.4})$$

To obtain the collective Hamiltonian, we need to consider extended adiabatic transformation

$$q = q^1 = f^1(\xi) + \frac{1}{2}f^{(1)1\alpha\beta}(\xi)\pi_\alpha\pi_\beta \quad (\text{II.5})$$

$$\xi^\alpha = g^\alpha(q) + \frac{1}{2}g^{(1)\alpha 11}(\xi)p_1p_1 \quad (\text{II.6})$$

and

$$p_1 = g_{,1}^\alpha \pi_\alpha \quad (\text{II.7})$$

$$\pi_\alpha = f_{,\alpha}^1 p_1, \quad (\text{II.8})$$

where the index 1 indicates the collective degree of freedom, and the comma indicates the partial derivative ($f_{,\alpha}^1 = \partial f^1 / \partial \xi^\alpha$). The canonical coordinates fulfill the canonicity

$$f_{,\alpha}^1 g_{,1}^\beta = \delta_\alpha^\beta, \quad f_{,\alpha}^1 g_{,1}^\alpha = 1. \quad (\text{II.9})$$

With these relations, collective potential $\bar{V}(q)$ and collective mass parameter $\bar{B}(q)$ can be transformed by

$$\bar{V}(q) = V(\xi) \quad (\text{II.10})$$

$$\bar{B}^{-1}(q) = f_{,\alpha}^1 B^{\alpha\beta}(\xi) f_{,\beta}^1, \quad (\text{II.11})$$

Before showing the ASCC basic equations, we consider the constants of motion in TDHFB dynamics. Since nuclei is self-bound systems without external potential, the ground state obtained from mean-field theory violates the symmetry (e.g. deformation, pairing). In such system, the constants of motion corresponding the Nambu-Goldstone (NG) mode emerges in TDHFB dynamics. Therefore, we are mostly interested in the systems with collective motion separated from NG mode.

We know that the most of conserved quantities, such as total angular momentum J and total particle number N , are not only expressed by one-body Hermitian operators, but also has real matrix elements in the quasi-particle basis. Such classical variable \mathcal{P} corresponding to the conserved quantity can be expanded as

$$\mathcal{P}(\xi, \pi) = f^I(\xi) + \frac{1}{2}f^{(1)I\alpha\beta}(\xi)\pi_\alpha\pi_\beta. \quad (\text{II.12})$$

The index I indicates the degree of freedom for NG mode. Since the conserved quantity must fulfill $\{\mathcal{P}, \mathcal{H}\}_{PB} = 0$, it leads

$$f_{,\alpha}^I B^{\alpha\beta} - f^{(1)I\alpha\beta} V_{,\alpha} = 0. \quad (\text{II.13})$$

Including the NG mode, $f^1(\xi)$ and $g^\alpha(q)$ are obtained by solving ASCC basic equations

$$\delta H_M(\xi, \pi) = 0 \quad (\text{II.14})$$

$$\tilde{B}^{\beta\gamma} V_{;\gamma\alpha} f_{,\beta}^1 = \omega^2 f_{,\alpha}^1, \quad \tilde{B}^{\beta\gamma} V_{;\gamma\alpha} g_{,1}^\alpha = \omega^2 g_{,1}^\beta. \quad (\text{II.15})$$

The first equation (II.14) is called moving-frame HFB equation. The moving-frame Hamiltonian \mathcal{H}_M with constraints on collective coordinate and constant of motion is

$$\mathcal{H}_M(\xi, \pi) = \mathcal{H}(\xi, \pi) - \lambda_1 q^1(\xi, \pi) - \lambda_I \mathcal{P}(\xi, \pi). \quad (\text{II.16})$$

The second equation (II.15) is called moving-frame QRPA equation. $\tilde{B}^{\alpha\beta}$ is the modified mass parameter

$$\begin{aligned} \tilde{B}^{\alpha\beta}(\xi) &= \frac{\partial^2 \mathcal{H}_M}{\partial \pi_\alpha \partial \pi_\beta} \\ &= B^{\alpha\beta}(\xi) - \lambda_I f^{(1)I\alpha\beta}(\xi) - \lambda_1 f^{(1)1\alpha\beta}(\xi). \end{aligned} \quad (\text{II.17})$$

and the covariant derivative $V_{;\gamma\alpha}$ is defined by

$$V_{;\alpha\beta} = V_{,\alpha\beta} - \Gamma_{\alpha\beta}^\gamma V_{,\gamma}, \quad (\text{II.18})$$

where the affine connection is $\Gamma_{\beta\gamma}^\alpha = \frac{1}{2}B^{\alpha\delta}(B_{\delta\beta,\gamma} + B_{\delta\gamma,\beta} - B_{\beta\gamma,\delta})$. If we assume that the collective coordinate q is geodesic, $\tilde{B}^{\beta\gamma}V_{;\gamma\alpha}$ can be simplified after several steps

$$\tilde{B}^{\alpha\gamma}V_{;\gamma\beta} = \tilde{B}^{\alpha\gamma}(V_{;\gamma\beta} - \lambda_I f_{;\gamma\beta}^I) + \frac{1}{2}\tilde{B}_{;\beta}^{\alpha\gamma}V_{;\gamma}. \quad (\text{II.19})$$

We discuss the practical solution to derive the one-dimensional collective coordinate. We neglect $f^{(1)1\alpha\beta}(\xi)$ because it is supposed to be negligibly small in the previous study. On the other hand, from (II.13) and (II.15), $f^{(1)1\alpha\beta}(\xi)$ is necessary information to promise $\tilde{B}^{\beta\gamma}V_{;\gamma\alpha}f_{;\beta}^I = 0$, which means zero mode. In most of case, we know the explicit form of $\mathcal{P}(\xi, \pi)$. The procedures to obtain the collective path are:

1. Find the energy minimum point in energy surface by solving (II.14) (normal HFB equation). We usually set $q^1 = 0$ at the energy minimum point.
2. Using (II.19), diagonalize (II.15) and choose the lowest mode basically.
3. The right eigenvector $g_{;1}^\alpha$ tell us the direction which system moves in energy surface. Use the relation $d\xi^\alpha = g_{;1}^\alpha dq^1$ to decide the neighborhood point $q^1 \rightarrow q^1 + dq^1$ in the collective path.
4. Using $f_{;\alpha}^1$, find the non-equilibrium energy minimum point by solving (II.14) at the neighborhood point. We usually use the constraint condition $dq = f_{;\alpha}^1(\xi^\alpha(q) - \xi^\alpha(q - dq))$ from the canonicity (II.9). After convergence, we diagonalize (II.15) and obtain the corrected $f_{;\alpha}^1$.
5. Iterate (4) until the convergence of $f_{;\alpha}^1$.
6. Iterate (2)~(5) to decide the collective path under the same direction in the energy surface.
7. Implement (2)~(6) for the opposite direction of the collective path in energy surface.

The scale of the collective coordinate is not unique because of the uncertainty of the eigenvectors in (II.15). To unify the scale, the simplest procedure is to keep the collective mass parameter $\tilde{B}^{-1}(q) = 1$ by renormalizing eigenvectors in (II.11).

B. Stationary-phase approximation to the path integral

In integrable system, we can apply the stationary phase approximation to the path integral (SPA) to obtain collective excited states. The concept of SPA is introduced in the previous study. Because the one-dimensional collective path extracted from TDHFB degrees of freedom is integrable system, SPA is supposed to be available for non-integrable system via ASCC.

Based on SPA, the k -th excited state $|\psi_k\rangle$ can be constructed by a periodic TDHFB trajectory

$$|\psi_k\rangle = \oint d\mu(Z^{(k)}) |Z^{(k)}\rangle e^{i\mathcal{T}[Z^{(k)}]/\hbar}. \quad (\text{II.20})$$

The integration indicates we integrate a periodic TDHFB trajectory for one period in TDHFB phase space. The invariant measure $d\mu(Z)$ is defined by the unity condition $\int d\mu(Z) |Z\rangle \langle Z| = 1$. The action integral \mathcal{T} is defined by

$$\mathcal{T}[Z] \equiv \int_0^t \langle Z(t') | i\hbar \frac{\partial}{\partial t'} | Z(t') \rangle dt'. \quad (\text{II.21})$$

We try to combine SPA with ASCC. The key point is to find the correspondence between TDHFB phase space and collective subspace in a TDHFB trajectory (See Fig. 1). We consider the time-dependent state vector $|Z(t)\rangle$ is in a collective subspace. With pairing correlation, $|Z(t)\rangle$ can be expressed as

$$|Z(t)\rangle = |\Phi, J; q, p\rangle = e^{-i\Phi\hat{J}} |J; q, p\rangle, \quad (\text{II.22})$$

where Φ is the total gauge angle and $J = N/2$ is the conjugate momentum corresponding total particle number. The second equal sign indicates an intrinsic state $|J; q, p\rangle$ rotates in the gauge space. Since $[H, J] = 0$, the classical Hamiltonian becomes

$$\begin{aligned} \mathcal{H} &= \langle \Phi, J; q, p | H | \Phi, J; q, p \rangle \\ &= \langle J; q, p | H | J; q, p \rangle \equiv \mathcal{H}_J(q, p) \end{aligned} \quad (\text{II.23})$$

has no dependence of Φ . Therefore, the classical Hamiltonian is the function of (q, p) in a fixed particle number system, and correspond to (II.4). From ASCC, we can obtain the static state vector at each point of q , namely $|J; q, p=0\rangle$. To construct $|J; q, p\rangle$, we use (II.8) at (q, p) which we want to know in the collective phase space. Usually, we are interested in the points $(q^{(k)}, p^{(k)})$ at the k -th TDHFB trajectory. Such k -th TDHFB trajectory is obtained from EBK quantization condition (k : integer)

$$\begin{aligned} \mathcal{T}_0[Z^{(k)}] &= \oint \langle Z^{(k)}(t') | i\hbar \frac{\partial}{\partial t'} | Z^{(k)}(t') \rangle dt' \\ &= \oint p^{(k)} dq^{(k)} = 2k\pi. \end{aligned} \quad (\text{II.24})$$

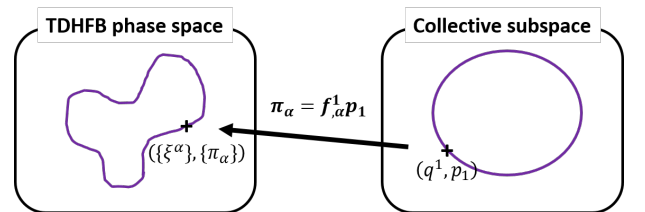


FIG. 1: For a TDHFB trajectory, the correspondence between TDHFB phase space and collective subspace.

The procedures to obtain excited states from SPA via ASCC are:

1. Obtain the one-dimensional collective coordinate from ASCC.
2. Using collective Hamiltonian, obtain k -th excitation energy and TDHFB trajectory under EBK quantization condition (II.24).
3. For k -th TDHFB trajectory, construct the state vector $|J; q, p\rangle$ by using (II.8).
4. Calculate action integral (III.22) in k -th TDHFB trajectory.
5. Using (II.20), obtain k -th excited state.

III. APPLICATION IN PAIRING MODEL

We study the low-lying excited 0^+ states in multi-level pairing model by applying SPA via ASCC. The Hamiltonian of the pairing model is given in terms of single-particle energies ϵ_l and the pairing strength g as

$$\begin{aligned} H &= \sum_l \epsilon_l n_l - g \sum_{l,l'} S_l^+ S_{l'}^- \\ &= \sum_l \epsilon_l (2S_l^0 + \Omega_l) - g S^+ S^-, \end{aligned} \quad (\text{III.1})$$

where we use the SU(2) quasi-spin operators, $\mathbf{S} = \sum_l \mathbf{S}_l$, with

$$S_l^0 = \frac{1}{2} \left(\sum_m a_{lm}^\dagger a_{lm} - \Omega_l \right), \quad (\text{III.2})$$

$$S_l^+ = \sum_{m>0} a_{lm}^\dagger a_{l\bar{m}}, \quad S_l^- = S_l^{+\dagger}. \quad (\text{III.3})$$

Each single-particle energy ϵ_l possesses $(2\Omega_l)$ -fold degeneracy ($\Omega_l = j_l + 1/2$) and $\sum_{m>0}$ indicates the summation over $m = 1/2, 3/2, \dots$, and $\Omega_l - 1/2$. The occupation number of each level l is given by $n_l = \sum_m a_{lm}^\dagger a_{lm} = 2S_l^0 + \Omega_l$. The quasi-spin operators satisfy the commutation relations

$$[S_l^0, S_{l'}^\pm] = \pm \delta_{ll'} S_l^\pm, \quad [S_l^+, S_{l'}^-] = 2\delta_{ll'} S_l^0. \quad (\text{III.4})$$

The magnitude of quasi-spin for each level is $S_l = \frac{1}{2}(\Omega_l - \nu_l)$, where ν_l is the seniority quantum number, namely the number of unpaired particle at each level l . In the present study, we only consider seniority zero states with $\nu = \sum_l \nu_l = 0$. The residual two-body interaction only consists of monopole pairing interaction which couples two particles to zero angular momentum. We obtain exact solutions either by solving Richardson equation [24–26] or by diagonalizing the Hamiltonian using the quasi-spin symmetry.

A. Classical form of TDHFB Hamiltonian

The coherent state for the seniority $\nu = 0$ states ($S_l = \Omega_l/2$) is constructed as

$$|Z(t)\rangle = \prod_l (1 + |Z_l(t)|^2)^{-\Omega_l/2} \exp[Z_l(t) S_l^+] |0\rangle \quad (\text{III.5})$$

where $|0\rangle$ is the vacuum (zero particle) state, $Z_l(t)$ are time-dependent complex variables which describe motion of the system. In the SU(2) quasi-spin representation, $|0\rangle = \prod_l |S_l, -S_l\rangle$. The coherent state $|Z(t)\rangle$ is a superposition of states with different particle numbers without unpaired particles. In the present pairing model, the coherent state is the same as the time-dependent BCS wave function with $Z_l(t) = v_l(t)/u_l(t)$, where $(u_l(t), v_l(t))$ are the time-dependent BCS u, v factors.

The TDHFB equation can be derived from the time-dependent variational principle (we set $\hbar = 1$),

$$\delta S = 0, \quad S \equiv \int \mathcal{L}(t) dt = \int \langle Z(t) | i \frac{\partial}{\partial t} - H | Z(t) \rangle dt. \quad (\text{III.6})$$

After transformation of the complex variables $Z_l = \tan \frac{\theta_l}{2} e^{-i\chi_l}$ ($0 \leq \theta \leq \pi$) and several steps of the derivation, the Lagrangian \mathcal{L} and the expectation value of Hamiltonian become

$$\mathcal{L}(t) = \sum_l \frac{\Omega_l}{2} (1 - \cos \theta_l) \dot{\chi}_l - \mathcal{H}(Z, Z^*), \quad (\text{III.7})$$

$$\begin{aligned} \mathcal{H}(Z, Z^*) &\equiv \langle Z | H | Z \rangle \\ &= \sum_l \epsilon_l \Omega_l (1 - \cos \theta_l) - \frac{g}{4} \sum_l \Omega_l [\Omega_l (1 - \cos^2 \theta_l) + (1 - \cos \theta_l)^2] \\ &\quad - \frac{g}{4} \sum_{l_1 \neq l_2} \Omega_{l_1} \Omega_{l_2} \sqrt{(1 - \cos^2 \theta_{l_1})(1 - \cos^2 \theta_{l_2})} e^{-i(\chi_{l_1} - \chi_{l_2})}. \end{aligned} \quad (\text{III.8})$$

Here, we choose χ_l as canonical coordinates. Their conjugate momenta are given by

$$j_l \equiv \frac{\partial \mathcal{L}}{\partial \dot{\chi}_l} = \frac{\Omega_l}{2} (1 - \cos \theta_l). \quad (\text{III.9})$$

χ_l represent a kind of gauge angle of each level, and j_l are related to the occupation number of each level, $2j_l = n_l$. Therefore, the TDHFB Hamiltonian can be represented by canonical variables $\mathcal{H}(Z, Z^*) = \mathcal{H}(\{\chi_l\}, \{j_l\})$, and the TDHFB equation is equivalent to the Hamilton's equation

$$\dot{\chi}_l = \frac{\partial \mathcal{H}}{\partial j_l}, \quad \dot{j}_l = -\frac{\partial \mathcal{H}}{\partial \chi_l}. \quad (\text{III.10})$$

B. Application into ASCC

In this subsection, we use (α, β, \dots) to describe the degrees of freedom instead of l to synchronize the notation with in Sec. II A. We construct 1D collective subspace from ASCC theory. Because the first order with respect to χ_α is zero in TDHFB Hamiltonian, we assume j^α as coordinates and χ_α as conjugate momenta. The canonical variables are $(j^\alpha, -\chi_\alpha)$ and fulfill $\{j^\alpha, -\chi_\beta\}_{PB} = \delta_\beta^\alpha$. We expand the classical Hamiltonian up to second order with respect to χ_α . The classical Hamiltonian becomes

$$\mathcal{H}(j, \chi) \approx V(j) + \frac{1}{2} B^{\alpha\beta}(j) \chi_\alpha \chi_\beta, \quad (\text{III.11})$$

where potential $V(j)$ and reciprocal mass parameter $B^{\alpha\beta}(j)$ are defined as

$$\begin{aligned} V(j) &= \mathcal{H}(\chi = 0, j) \\ &= \sum_{\alpha} 2\epsilon_{\alpha} j^{\alpha} - g \sum_{\alpha} \left(\Omega_{\alpha} j^{\alpha} - (j^{\alpha})^2 + \frac{(j^{\alpha})^2}{\Omega_{\alpha}} \right) \\ &\quad - g \sum_{\alpha \neq \beta} \sqrt{j^{\alpha} j^{\beta} (\Omega_{\alpha} - j^{\alpha})(\Omega_{\beta} - j^{\beta})} \quad (\text{III.12}) \end{aligned}$$

$$\begin{aligned} B^{\alpha\beta}(j) &= \frac{\partial^2 \mathcal{H}}{\partial \chi_{\alpha} \partial \chi_{\beta}} \Big|_{\chi=0} \\ &= \begin{cases} 2g \sum_{\gamma \neq \alpha} \sqrt{j^{\gamma} j^{\alpha} (\Omega_{\gamma} - j^{\gamma})(\Omega_{\alpha} - j^{\alpha})} & (\alpha = \beta) \\ -2g \sqrt{j^{\alpha} j^{\beta} (\Omega_{\alpha} - j^{\alpha})(\Omega_{\beta} - j^{\beta})} & (\alpha \neq \beta) \end{cases} \quad (\text{III.13}) \end{aligned}$$

where

Using the TDHFB Hamiltonian, we can apply ASCC explained in Sec. II A by replacing $\xi \rightarrow j$ and $\pi \rightarrow -\chi$.

We consider the treatment for the constant of motion in pairing model. In the TDHFB Hamiltonian, there is no dependence about the total gauge angle

$$\Phi = \frac{1}{L} \sum_{\alpha} \chi_{\alpha}. \quad (\text{III.14})$$

It indicates the conjugate momentum

$$J \equiv \frac{\partial \mathcal{L}}{\partial \Phi} = \sum_{\alpha} j^{\alpha} = \frac{N}{2} \quad (\text{III.15})$$

is conserved quantity. From this equation, we can find J is not dependent of χ , which means $f^{(1)I\alpha\beta}$ in (II.12) is zero. Therefore, $B^{\beta\gamma} V_{;\gamma\alpha} f_{,\beta}^I = 0$ is promised exactly. Also, the second derivative of J with respect to j vanishes, which indicates $f_{,\gamma\beta}^I$ in (II.19) is zero. It indicates the chemical potential $\lambda_I(q)$ is not necessary information to calculate the matrix element in moving-frame QRPA equation.

With the properties of the constant of motion, we discuss the practical solution of ASCC in pairing model. If we ignore the higher order term $f^{(1)1\alpha\beta}$, we can practice local harmonic equation (LHE)

$$B^{\beta\gamma} V_{;\gamma\alpha} f_{,\beta}^1 = \omega^2 f_{,\alpha}^1, \quad B^{\beta\gamma} V_{;\gamma\alpha} g_{,1}^{\alpha} = \omega^2 g_{,1}^{\beta}, \quad (\text{III.16})$$

which simplifies the moving-frame QRPA equation (II.15) by replacing $\tilde{B}^{\beta\gamma}$ into $B^{\beta\gamma}$. Under (III.16), the eigenvalue of spurious mode corresponding pairing rotation is exact zero. To guarantee the state vectors $|Z(q)\rangle$ are in the same total gauge angle $\Phi(q) = -\frac{1}{L} p_1 \sum_{\alpha} f_{,\alpha}^1 = 0$, we correct the eigenvectors by

$$f_{,\alpha}^1 \rightarrow f_{,\alpha}^1 - \frac{1}{L} \sum_{\beta} f_{,\beta}^1 \quad (\text{III.17})$$

after solving (III.16) at each point of q .

C. Application into SPA

We derive the explicit form of excited states in (II.20). From (II.22) and (III.15), the state vector $|\Phi, J; q, p\rangle$ becomes

$$|\Phi, J; q, p\rangle = \sum_{\{j_l\}} e^{-i\Phi \sum_l j_l} |J; q, p\rangle. \quad (\text{III.18})$$

Here, $|J; q, p\rangle$ can be expanded in SU(2) quasispin basis

$$|J; q, p\rangle = \sum_{\{j_l\}} A_{j_l}(q, p) |\cdots; S_l, -S_l + k_l, \cdots\rangle, \quad (\text{III.19})$$

$$\begin{aligned} A_{j_l}(q, p) &= \prod_l \left(\frac{1 - \cos \theta_l}{2} \right)^{j_l/2} \left(\frac{1 + \cos \theta_l}{2} \right)^{(\Omega_l - j_l)/2} \\ &\quad \times \sqrt{\frac{(\Omega_l)!}{j_l! (\Omega_l - j_l)!}} e^{-ij_l \chi_l} \quad (\text{III.20}) \end{aligned}$$

is in fixed gauge angle ($\Phi = 0$).

Due to J is conserved quantity, the action integral can be divided into two terms

$$\mathcal{T}(\Phi, J; q, p) = \mathcal{T}_{\text{intr}}(t) + J\Phi, \quad (\text{III.21})$$

where the intrinsic action integral $\mathcal{T}_{\text{intr}}(t)$ becomes

$$\begin{aligned} \mathcal{T}_{\text{intr}}(t) &= \int \langle J; q, p | i \frac{\partial}{\partial t} | J; q, p \rangle dt \\ &= \int \sum_l j_l d\chi_l. \quad (\text{III.22}) \end{aligned}$$

The important point is $\mathcal{T}_{\text{intr}}(t) \neq \int p dq$ at each t . For closed TDHFB trajectory, only $\mathcal{T}_{\text{intr}}(t)$ contributes to the excited states. In SU(2) representation, the invariant measure is

$$\begin{aligned} d\mu(Z) &= \prod_l \frac{\Omega_l + 1}{\pi} (1 + |Z_l|^2)^{-2} d\text{Re} Z d\text{Im} Z \\ &= \prod_l \frac{\Omega_l + 1}{4\pi} d\cos \theta_l d\chi_l \\ &= \prod_l \frac{-(1 + \Omega_l^{-1})}{2\pi} d\chi_l dj_l \\ &= \left[\prod_l \frac{-(1 + \Omega_l^{-1})}{2\pi} \right] d\Phi dJ dq dp \\ &\quad \times dQ_1 \cdots dQ_{l-2} dP_1 \cdots dP_{l-2} \quad (\text{III.23}) \end{aligned}$$

where (Q_i, P_i) are the other canonical variables decoupled from the collective coordinates. From the third line to the forth line, we used that Jacobian equals one in canonical transformation. The part of the invariant measure which contributes to the excited states is

$$d\mu(\Phi, J; q, p) \propto d\Phi dJ dq dp = d\Phi dJ dE dt. \quad (\text{III.24})$$

Under EBK quantization condition (II.24), the k -th excited state becomes

$$\begin{aligned}
|\tilde{\phi}_k\rangle &\propto \oint d\Phi \oint dt |\Phi, J; q, p\rangle e^{i\mathcal{T}(\Phi, J; q, p)} \\
&= \sum_{\{j_l\}} \oint d\Phi e^{i(J - \sum_l j_l)\Phi} \\
&\quad \times \oint dt e^{i\mathcal{T}_{\text{intr}}(t)} A_{j_l}(q, p) |\cdots; S_l, -S_l + j_l, \cdots\rangle \\
&\equiv \sum_{\{j_l\} \in (\sum_{j_l} = J)} C_{j_l} |\cdots; S_l, -S_l + j_l, \cdots\rangle \quad (\text{III.25})
\end{aligned}$$

where

$$C_{j_l} = \oint dt e^{i\mathcal{T}_{\text{intr}}(t)} A_{j_l}(q(t), p(t)). \quad (\text{III.26})$$

The definition of wave function in SPA can also be extended into ground state. The ground state is constructed by only energy minimum point in TDHFB phase space. In the energy minimum point, $|\Phi, J; q, p\rangle = |\text{HFB}\rangle$. Therefore, (III.25) becomes

$$|\tilde{\phi}_{g.s.}\rangle \propto \sum_{\{j_l\}} \oint d\Phi e^{i(J - \sum_l j_l)\Phi} |\text{HFB}\rangle, \quad (\text{III.27})$$

which is identical to the wave function of the particle number projection for HFB state.

IV. RESULTS

We apply ASCC+SPA to study the multi-level system in pairing model. The TDHFB degrees of freedom equals the number of single particle levels, including the constant of motion (pairing rotation). We consider various systems, two-level system, three-level system, and Pb isotope system in each subsection respectively. Next, we discuss the dynamics in non-integrable (more than three-level) system.

A. Confirmation in one-dimensional TDHFB system

The two-level system corresponds to one-dimensional TDHFB system after decoupling the global gauge angle Φ . We can obtain the obvious collective path from ASCC. The dynamics is exactly identical with adiabatic TDHFB (ATDHFB). We confirm that whether ASCC is identical to one-dimensional ATDHFB, and compare the difference with TDHFB, in numerical calculation.

In two-level system, the classical Hamiltonian in (III.8)

is

$$\begin{aligned}
\mathcal{H} &= \sum_{l=1,2} \epsilon_l \Omega_l (1 - \cos \theta_l) \\
&\quad - \frac{g}{4} \sum_{l=1,2} \Omega_l [\Omega_l (1 - \cos^2 \theta_l) + (1 - \cos \theta_l)^2] \\
&\quad - \frac{g}{2} \Omega_1 \Omega_2 \sqrt{(1 - \cos^2 \theta_{l_1})(1 - \cos^2 \theta_{l_2})} \cos(\chi_2 - \chi_1). \quad (\text{IV.1})
\end{aligned}$$

If we define the canonical coordinate $\phi = \chi_2 - \chi_1$, it attributes to one-dimensional system. The conjugate momentum is $j = \frac{\partial \mathcal{L}}{\partial \phi} = \{\Omega_2(1 - \cos \theta_2) - \Omega_1(1 - \cos \theta_1)\}/4$. The ATDHFB indicates that the Hamiltonian can be expanded up to second order with respect to ϕ

$$\mathcal{H}(\phi, j) \approx V(j) + \frac{1}{2} B^{-1}(j) \phi^2, \quad (\text{IV.2})$$

where $V(j) = \mathcal{H}(\phi = 0, j)$ and $B^{-1}(j) = \frac{\partial^2 \mathcal{H}}{\partial \phi^2} \Big|_{\phi=0}$. We know that the BCS ground state corresponds to the potential minimum point with $\phi = 0$. If the pairing correlation is strong enough to bind the excited states in the collective potential, the adiabatic approximation is expected to be well because the states are localized in small ϕ region.

We study the system with equal degeneracy $\Omega_1 = \Omega_2 = 8$, $g/(\epsilon_2 - \epsilon_1) = 0.2$, and $N = 16$. In ASCC calculation, we set the mesh size of collective coordinate $dq = 0.01$. We compared the results of $|0_2^+\rangle$ and $|0_3^+\rangle$ in three different calculations. Fig. 2 and Fig. 3 correspond to the classical informations, which are classical trajectories in phase space and action integral \mathcal{T} as a function of time t . All of the mesh points obtained from ASCC are on the trajectories obtained from ATDHFB. For $|0_2^+\rangle$, the closed trajectory is well localized in the phase space and TDHFB calculation is almost the same as ASCC and ATDHFB calculations. For $|0_3^+\rangle$, the trajectory is still closed but near the transition point between closed trajectory and open trajectory. We can find ASCC and ATDHFB calculations have a small deviation from TDHFB calculation. The obtained excited 0^+ states from SPA are shown in Fig. 4. We show the occupation probability which is decomposed into $2n$ -particle- $2n$ -hole components. The results from ATDHFB and ASCC are identical within numerical error. Also, TDHFB calculation is very close to other two calculations.

Comparing with one-dimensional TDHFB calculation, we confirmed we succeed to describe the bound collective excited states by ASCC+SPA. For the bound states, whether the adiabatic approximation included or not hardly has influence. Even for the weakly bound states, the adiabatic approximation is reasonable approximation.

B. Three-level system

The simplest non-integrable system is three-level system. We have one trivial motion and two time-dependent

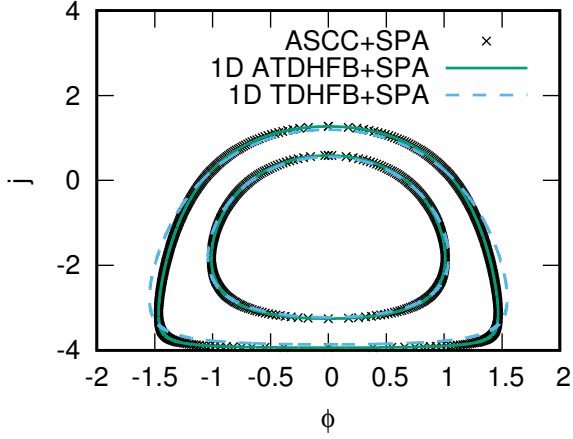


FIG. 2: Classical trajectories of $|0_2^+\rangle$ and $|0_3^+\rangle$ in two-dimensional phase space. The domain of phase space is $-\pi \leq \phi < \pi$, $-4 \leq j \leq 4$. Cross points, solid lines, and dashed lines correspond to the results from ASCC+SPA, one-dimensional ATDHFB+SPA, and one-dimensional TDHFB+SPA, respectively. In ASCC+SPA calculation, each cross point corresponds to each mesh point from ASCC calculation.

degrees of freedom. We study the system with $\Omega_1 = \Omega_2 = \Omega_3 = 8$, $\epsilon_1 = -1$, $\epsilon_2 = 0$, $\epsilon_3 = 1.5$, and $g = 0.2$. The phase transition occurs at $g_c = 0.058$ when $N = 2\Omega_1 = 16$. We consider the even particle number chain from $N = 14$ to $N = 24$.

From moving-frame QRPA equation, we obtain three modes along the collective path (Fig. 5). Except zero mode, we choose the lowest mode as collective motion. Fig. 6 and Fig. 7 are occupation number in each single-particle level and collective potential in the collective path, respectively. We can find the occupation numbers become to integer at both end points. Furthermore, Hartree-Fock states always emerge at one of the end point.

Based on the information from ASCC calculation, we can obtain the excited states from SPA. Table I shows the excitation energies of first and second excited states in the collective subspace. Up to the second excitation, all of the energies are in their energy pockets shown in Fig. 7. Comparing the result from ASCC+SPA with exact solution, we can find all of the values are nicely reproduced. The slightly difference is that the values from ASCC+SPA are about 5% smaller than exact solution. Using the wave function of excited states, the pair additional transition strength is shown in Fig. 8. For intraband transition, comparing ASCC+SPA with exact solution, $B(P_{ad}; 0_1^+ \rightarrow 0_1^+)$ are almost identical and $B(P_{ad}; 0_2^+ \rightarrow 0_2^+)$ are about 10% ~ 20% small. For interband transition, the strength from ASCC+SPA is much smaller than exact solution. It is difficult to reproduce the absolute value of exact solution. However, because the pairing correlation is enough strong in this case, the strength of intraband transition is dominant

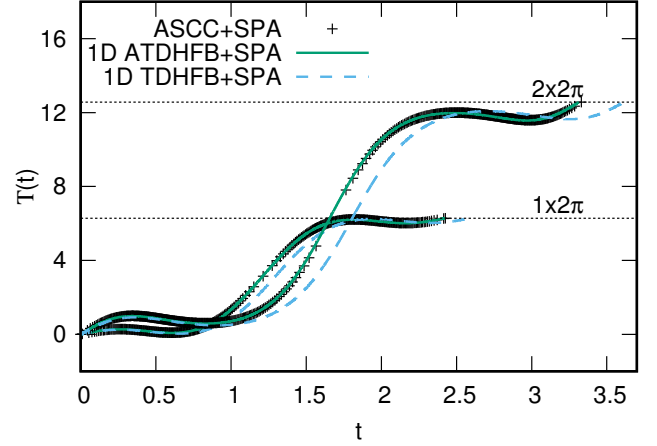


FIG. 3: Action integrals of $|0_2^+\rangle$ and $|0_3^+\rangle$ with respect to time t . Cross points, solid lines, and dashed lines correspond to the results from ASCC+SPA, one-dimensional ATDHFB+SPA, and one-dimensional TDHFB+SPA, respectively. Dotted lines are the values correspond to EBK quantization condition for $|0_2^+\rangle$ and $|0_3^+\rangle$. Based on Fig. 2, we calculated the action integrals on each trajectory from $(\phi, j) = (0, j_{\max})$ in clockwise direction.

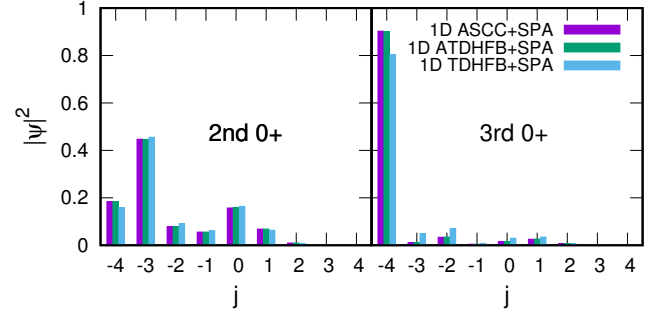


FIG. 4: Occupation probabilities of $|0_2^+\rangle$ and $|0_3^+\rangle$ as a function of j . The two vertical bars at each j from the left to the right represent the squared components of the wave functions from ASCC+SPA, ATDHFB+SPA and TDHFB+SPA calculations, respectively. The left end of the horizontal axis at $j = j_{\min}$ corresponds to a component with $(n_1, n_2) = (N, 0)$. The next at $j = j_{\min} + 1$ corresponds to the one with $(n_1, n_2) = (N - 2, 2)$, and so on.

compared with interband transition. We can find that $B(P_{ad}; 0_1^+ \rightarrow 0_2^+)$ and $B(P_{ad}; 0_2^+ \rightarrow 0_1^+)$ are only about 1% of $B(P_{ad}; 0_1^+ \rightarrow 0_1^+)$ and $B(P_{ad}; 0_2^+ \rightarrow 0_2^+)$. Therefore, the interband transition can be regarded as reasonable. From all above results, we can conclude that ASCC+SPA reproduces exact solution quantitatively.

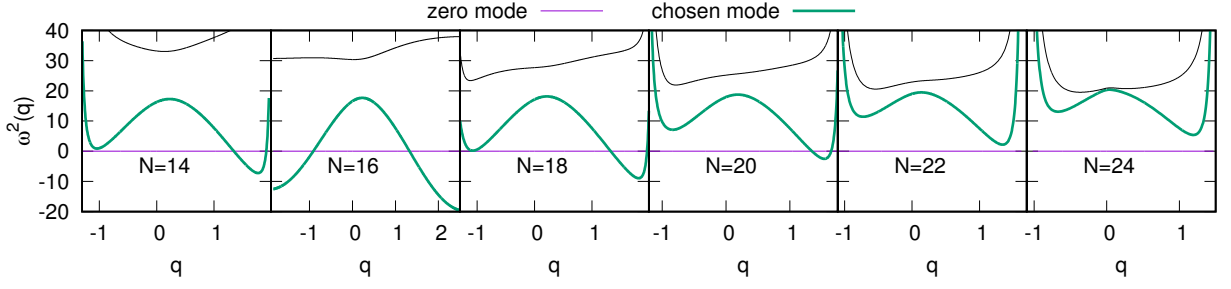


FIG. 5: Eigenvalues of moving-frame QRPA equation with respect to the collective coordinate q , from $N = 14$ to $N = 24$. Purple lines are spurious modes and green lines are chosen modes corresponding to the collective coordinate. In each panel, both edges correspond to the end points of the collective coordinate.

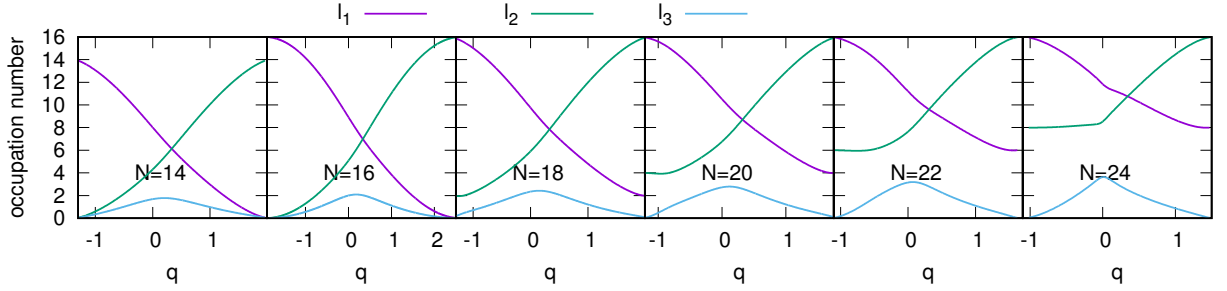


FIG. 6: Occupation numbers in each single-particle level with respect to the collective coordinate q , from $N = 14$ to $N = 24$. At the left end point of the collective coordinate in each panel, the configurations correspond to Hartree-Fock states.

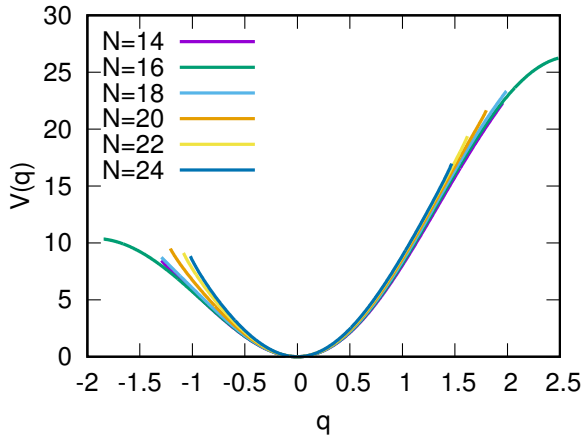


FIG. 7: Collective potential obtained from ASCC. We adjusted the energy minimum point as $V = 0$.

We need to discuss about the second excited state in the collective path corresponds to not $|0_3^+\rangle$ and others, but $|0_4^+\rangle$. In pair additional transition $B(P_{\text{ad}}; k \rightarrow k')$ from exact solution, $B(P_{\text{ad}}; 0_2^+ \rightarrow 0_3^+)$ is 10 \sim 100 times smaller than $B(P_{\text{ad}}; 0_1^+ \rightarrow 0_3^+)$, and $B(P_{\text{ad}}; 0_1^+ \rightarrow 0_2^+)$ is in the same order with $B(P_{\text{ad}}; 0_1^+ \rightarrow 0_3^+)$. It in-

dicates that $|0_3^+\rangle$ is also one-phonon state which belongs to the other collective path (black line in Fig. 5). About two-phonon states, we can easily find the candidates of two-phonon states from excitation energies and $B(P_{\text{ad}}; 0_1^+ \rightarrow 0_{ex}^+)$. In the candidates, $|0_4^+\rangle$ is the lowest two-phonon state and $B(P_{\text{ad}}; 0_2^+ \rightarrow 0_4^+)$ is much larger than $B(P_{\text{ad}}; 0_3^+ \rightarrow 0_4^+)$. Therefore, $|0_4^+\rangle$ is considered to be most appropriate corresponding to the second excited state in ASCC+SPA calculation.

| | N | 14 | 16 | 18 | 20 | 22 | 24 |
|--------------------|----------|------|------|------|------|------|------|
| 0_2^+ one phonon | Exact | 4.09 | 4.13 | 4.20 | 4.30 | 4.44 | 4.60 |
| | ASCC+SPA | 3.87 | 3.90 | 3.97 | 4.09 | 4.23 | 4.33 |
| 0_4^+ two phonon | Exact | 7.65 | 7.71 | 7.88 | 8.15 | 8.49 | 8.74 |
| | ASCC+SPA | 7.42 | 7.42 | 7.60 | 7.92 | 8.26 | 8.47 |

TABLE I: Excitation energies of one-phonon and two-phonon states from exact solution and ASCC+SPA calculation. In a chosen collective subspace, one-phonon and two-phonon states correspond to the first and second excitation, respectively. In the whole Hilbert space, one-phonon and two-phonon states correspond to $|0_2^+\rangle$ and $|0_4^+\rangle$, respectively.

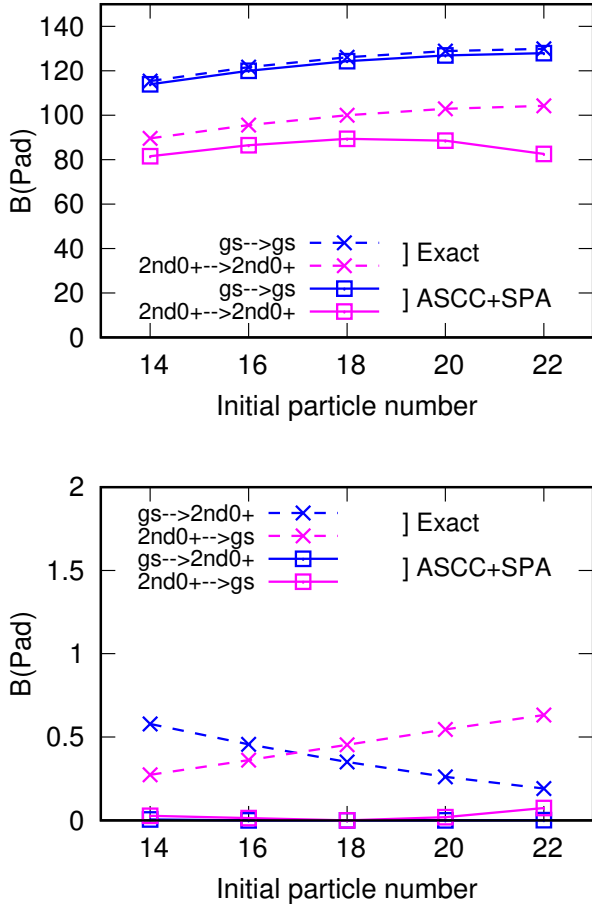


FIG. 8: The strength of pair additional transition $B(P_{\text{ad}}; k \rightarrow k') = |\langle N+2, k' | S^+ | N, k \rangle|^2$, from $N = 14$ to $N = 22$. Dashed lines are exact solution and solid lines are ASCC+SPA calculation. Horizontal line shows the particle number of the initial states. Upper panel shows the intraband transitions of $|0_1^+\rangle \rightarrow |0_1^+\rangle$ and $|0_2^+\rangle \rightarrow |0_2^+\rangle$, while lower panel shows the interband transition of $|0_1^+\rangle \rightarrow |0_2^+\rangle$ and $|0_2^+\rangle \rightarrow |0_1^+\rangle$.

C. Pb isotopes

With pairing model, we study neutron's pairing vibration in Pb isotope. We prepare the neutron's single-particle level between the magic number 82 and 126 (Table II). The coupling constant $g = 0.138(\text{MeV})$ is determined to reproduce the experimental pairing gap $\Delta(N) = \frac{(-1)^{N+1}}{2}(B(N+1) - 2B(N) + B(N-1))$ of ^{192}Pb . We consider the even-even system from ^{188}Pb to ^{194}Pb .

We have six TDHFB degrees of freedom in the system. Fig. 9 shows the eigenvalue of moving-frame QRPA equation. We can find there are one spurious mode and five vibrational modes. The collective modes we focus on did not cross with other modes in all panels, while the spacings of the collective modes and the second vibrational

| orbit | $h_{9/2}$ | $f_{7/2}$ | $i_{13/2}$ | $p_{3/2}$ | $f_{5/2}$ | $p_{1/2}$ |
|-------------|-----------|-----------|------------|-----------|-----------|-----------|
| energy(MeV) | -10.94 | -10.69 | -8.74 | -8.44 | -8.16 | -7.45 |

TABLE II: Single-particle levels of Pb isotopes used in the calculation. The orbits are obtained from spherical Woods-Saxon potential with spin-orbit coupling.

modes are small, especially for ^{194}Pb . Under the chosen collective modes, the occupation number is shown in Fig. 10. As with three-level system, the left end points correspond to HF state in all panels. The last neutrons are in $i_{13/2}$ from ^{188}Pb to ^{194}Pb . In the collective path, we can find $i_{13/2}$ and $p_{3/2}$ orbits change significantly, while other orbits don't change so much. The collective potential for each isotope is shown in Fig. 11. The depths of them are about $2.5 \sim 3.5(\text{MeV})$ only enough to bind $|0_2^+\rangle$, one-phonon states. We can consider that the collectivity of pairing is small for excited states, even though their ground states are superfluid states.

We show the results of $|0_2^+\rangle$, one-phonon state in the collective coordinate, from SPA. Table II shows the excitation energy. The value is nothing to do with experimental value because pairing model is too simple to describe realistic nuclear interaction. We are only interested in the comparison between exact solution and ASCC+SPA. We can find the excitation energy from ASCC+SPA reproduce the exact solution as well as in three-level system. The pair additional transition strength is shown in Fig. 12. The feature is similar to the case in three-level system, dominant intraband transition and the accuracy from ASCC+SPA. The deviation of $B(P_{\text{ad}}; 0_2^+ \rightarrow 0_2^+)$ has about 25% deficiency compared with exact solution. Therefore, ASCC+SPA gives reasonable results in realistic single-particle level systems.

| | ^{186}Pb | ^{188}Pb | ^{190}Pb | ^{192}Pb | ^{194}Pb | ^{196}Pb |
|----------|-------------------|-------------------|-------------------|-------------------|-------------------|-------------------|
| Exact | 2.58 | 2.44 | 2.34 | 2.25 | 2.20 | 2.15 |
| ASCC+SPA | unbound | 2.31 | 2.21 | 2.12 | 2.04 | unbound |

TABLE III: The same as Table. I but for Pb isotopes. The energies are given in units of MeV.

Finally, we discuss about the validity of the collective treatment of the pairing. We know that the 5D collective model described by the quadrupole deformation parameters $\alpha_{2\mu}(\mu = \pm 2, \pm 1, 0)$ is widely applied to analyze experimental data. As with the 5D collective model, pairing can also be supposed as a sort of deformation. The collective model is described by the pair deformation parameters pairing gap Δ and global gauge angle Φ . The utilization of the collective model for nuclear pairing dynamics was done in several references[. In our previous study, however, we find that the pairing gap Δ is not proper to be the collective coordinate in two-level pairing model[. In multi-level system, we can investigate the relations between the pairing gap and the collective

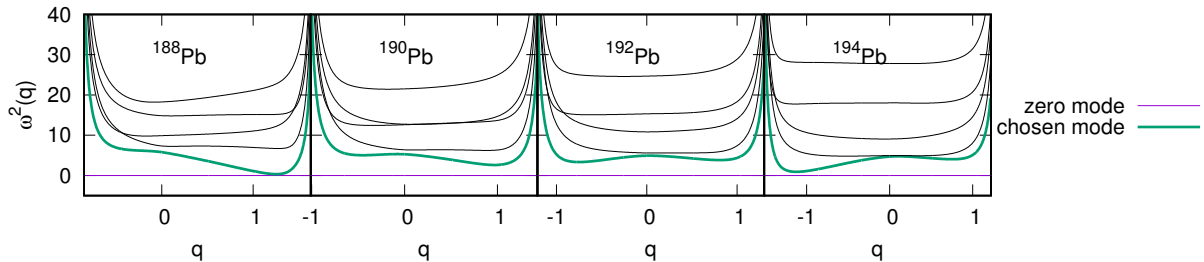


FIG. 9: The same as Fig. 5 but for Pb isotopes.

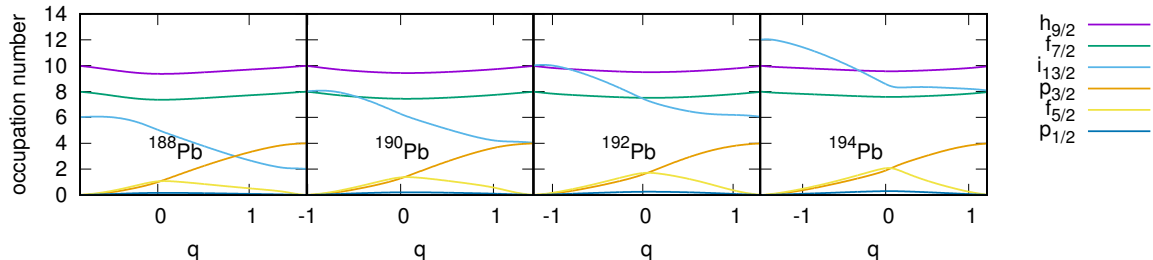


FIG. 10: The same as Fig. 6 but for Pb isotopes.

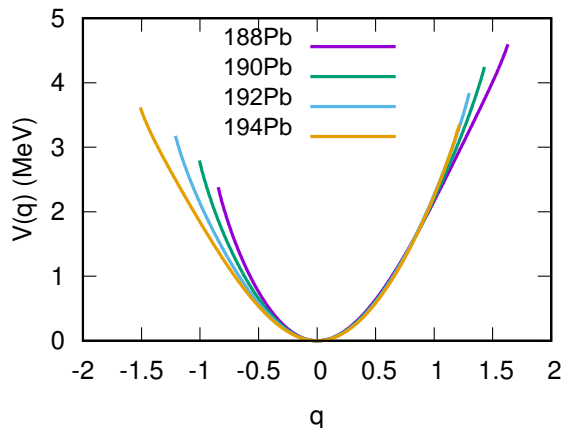


FIG. 11: The same as Fig. 7 but for Pb isotopes.

coordinate. The pairing gap Δ is defined as

$$\begin{aligned} \Delta(q) &\equiv g \langle \Phi, J; q, p | S^- | \Phi, J; q, p \rangle \big|_{\Phi=p=0} \\ &= g \sum_l \sqrt{j_l(\Omega_l - j_l)}. \end{aligned} \quad (\text{IV.3})$$

Fig. 13 shows the pairing gap of Δ in ^{192}Pb as a function of the collective coordinate q . We can see that the peak is near $q = 0$ and both end points have small values. Because only one orbit near the Fermi energy ($i_{13/2}$ orbit for both end points) contributes the value of pairing gap, the value at both end points are small compared with the

value around the ground state. There is no one-to-one correspondence between Δ and q not only in ^{192}Pb , but also in all multi-level systems. Therefore, the pairing gap Δ cannot properly describe the pairing dynamics.

V. CONCLUSION AND DISCUSSION

Based on our previous work which demonstrated the accuracy of SPA for the requantization of TDHFB dynamics, we considered the application of SPA to non-integrable system. The one of the possible way to extend SPA into non-integrable system is to combine with ASCC. We constructed the theoretical framework of ASCC+SPA for bound states, which is bound in the collective potential from ASCC.

We applied ASCC+SPA into multi-level pairing model. Because the global gauge angle Φ is a cyclic variable, the simplest non-integrable system is three level system. We investigated three level system and more realistic system, neutron's single-particle levels from Pb isotope. In both cases, the low-lying excited 0^+ states from ASCC+SPA reproduce exact solution well not only for excitation energies but also for wave functions. In ASCC+SPA, the pair transition calculation has no difficulty because we don't need to requantize the pair transition operators. This point overcomes the disadvantage in canonical requantization.

While the basic theoretical framework of ASCC+SPA was constructed, there are several problems remaining. Up to now, ASCC+SPA is only available when the ex-

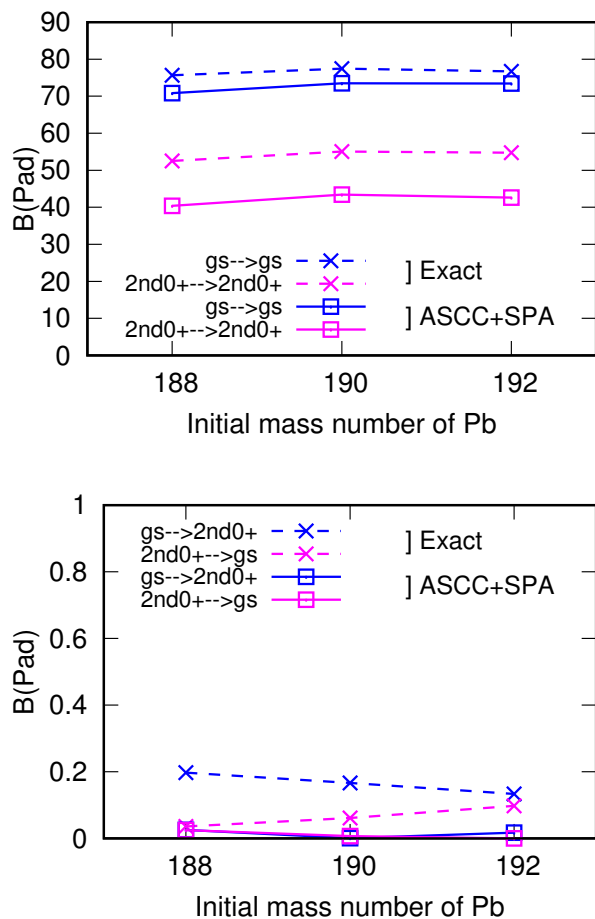


FIG. 12: The same as Fig. 8 but for Pb isotopes.

cited states are bound in the pocket of collective potential (See Fig. 7 and 11). For example, we cannot calculate $|0_2^+\rangle$ in ^{186}Pb because the potential is too shallow to bound the excited state. The difficulty for the application to the unbound states is that the wave function from SPA is not stationary state because the classical trajectory in phase space is not periodic. It is necessary to find some proper boundary conditions in the collective subspace. The second problem is about the crossing of the eigenvalues from moving-frame QRPA equation in the collective path. No problem occurs when two completely

orthogonal modes crossing, such as rotational mode and vibrational mode (e.g. $N=14,16,18,20$ in Fig. 5). However, if two vibrational modes not orthogonal with each other become the same eigenvalues, the ASCC calculation stops. Actually, the two eigenvalues become complex conjugate values and the next mesh point of collective path cannot be decided properly. Such case is occurred in ^{196}Pb . The eigenvalues crossing problem supposed to be the rare case because ^{196}Pb system is the only case including the previous studies about the application of ASCC. In addition, we need to consider the multi energy minimum pockets in the collective potential [21, 22]. Such case doesn't appear in pairing model. When the ex-

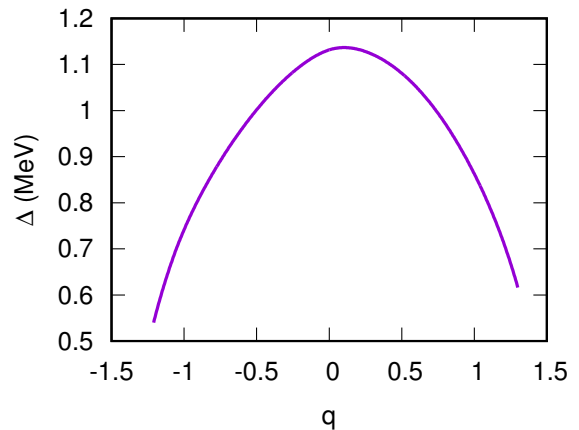


FIG. 13: Pairing gap as a function of collective coordinate in ^{192}Pb .

citation energy is below the multi minimum pocket, the EBK quantization condition is not unique. With these problems, the theoretical framework of ASCC+SPA need to be developed in the next step.

ACKNOWLEDGMENTS

This work is supported in part by Interdisciplinary Computational Science Program in CCS, University of Tsukuba, and by JSPS-NSFC Bilateral Program for Joint Research Project on Nuclear mass and life for unravelling mysteries of r-process.

-
- [1] P. Ring and P. Schuck, *The nuclear many-body problems*, Texts and monographs in physics (Springer-Verlag, New York, 1980).
 - [2] D. Brink and R. A. Broglia, *Nuclear Superfluidity, Pairing in Finite Systems* (Cambridge University Press, Cambridge, 2005).
 - [3] K. Heyde and J. L. Wood, Rev. Mod. Phys. **83**, 1467 (2011).
 - [4] P. E. Garrett, J. Phys. G **27**, R1 (2001).
 - [5] T. Nakatsukasa, K. Matsuyanagi, M. Matsuo, and K. Yabana, Rev. Mod. Phys. **88**, 045004 (2016).
 - [6] J. W. Negele, Rev. Mod. Phys. **54**, 913 (1982).
 - [7] S. Levit, Phys. Rev. C **21**, 1594 (1980).
 - [8] S. Levit, J. W. Negele, and Z. Paltiel, Phys. Rev. C **21**, 1603 (1980).
 - [9] H. Reinhardt, Nucl. Phys. A **346**, 1 (1980).
 - [10] H. Kuratsuji and T. Suzuki, Phys. Lett. B **92**, 19 (1980).
 - [11] H. Kuratsuji, Prog. Theor. Phys. **65**, 224 (1981).
 - [12] D. Bès, R. Broglia, R. Perazzo, and K. Kumar, Nucl. Phys. A **143**, 1 (1970).

- [13] A. Gózdź, K. Pomorski, M. Brack, and E. Werner, Nucl. Phys. A **442**, 50 (1985).
- [14] K. Zajac, L. Prochniak, K. Pomorski, S. G. Rohozinski, and J. Srebrny, Nucl. Phys. A **653**, 71 (1999).
- [15] K. Pomorski, Int. J. Mod. Phys. E. **16**, 237 (2007).
- [16] F. Ni and T. Nakatsukasa, Phys. Rev. C **97**, 044310 (2018).
- [17] T. Suzuki and Y. Mizobuchi, Prog. Theor. Phys, **79**, 480 (1988).
- [18] M. Matsuo, T. Nakatsukasa, and K. Matsuyanagi, Prog. Theor. Phys. **103**, 959 (2000).
- [19] T. Marumori, T. Maskawa, F. Sakata, and A. Kuriyama, Prog. Theor. Phys. **64**, 1294 (1980).
- [20] K. Masato, N. Takashi, M. Masayuki, and M. Kenichi, Prog. Theor. Phys. **113**, 129 (2005).
- [21] H. Nobuo, N. Takashi, M. Masayuki, and M. Kenichi, Prog. Theor. Phys. **117**, 451 (2007).
- [22] H. Nobuo, N. Takashi, M. Masayuki, and M. Kenichi, Prog. Theor. Phys. **119** (2008).
- [23] T. Nakatsukasa, Prog. Theor. Exp. Phys. **01A207** (2012).
- [24] R. W. Richardson, Phys. Lett. **3**, 277 (1963).
- [25] R. W. Richardson and N. Sherman, Nucl. Phys. **52**, 221 (1964).
- [26] R. W. Richardson and N. Sherman, Nucl. Phys. **52**, 353 (1964).